Available online at www.sciencedirect.com

SciVerse ScienceDirect

Procedia Environmental Sciences 19 (2013) 701 – 710

Procedia Environmental Sciences

Four Decades of Progress in Monitoring and Modeling Processes in the Soil-Plant-Atmosphere System: Applications and Challenges

Dielectric response of a variable saturated soil contaminated by Non-Aqueous Phase Liquids (NAPLs)

A. Comegna[a*], A. Coppola[b], G. Dragonetti[c], A. Sommella[d]

[a]*School of Agricultural Forestry Food and Environmental Sciences (SAFE), University of Basilicata, Potenza, Italy, (email: alessandro.comegna@unibas.it).*
[b]*Department of European and Mediterranean Cultures-Architecture, Environment, Cultural Heritage (DiCEM), Hydraulics and Hydrology Division, University of Basilicata, Matera, Italy.*

[c]*Institute for Mediterranean Agricultural and Forestry Systems (ISAFOM), National Research Council (CNR), Ercolano (NA), Italy.*
[d]*Division of Water Resources Management, University of Naples "Federico II", Italy*

Abstract

In recent years, several studies have been conducted both in saturated and unsaturated soils to detect non-aqueous phase liquid (NAPL) hydrocarbon contamination in soils and groundwater by means of the time domain reflectometry (TDR) technique. This technique is widely used for measuring the dielectric permittivity and bulk electrical conductivity of multiphase systems. Only accurate knowledge of the dielectric response of soil matrix-water-NAPL (saturated condition) or soil matrix-air-water-NAPL (unsaturated condition) systems can allow the volumetric NAPL content (θ_{NAPL}) to be determined in the soil. This paper investigates the influence of NAPL contamination (corn oil, a non-volatile and non-toxic NAPL, was used) on TDR measurement in a volcanic soil, relating dielectric permittivity of the multiphase soil system to volumetric fluid content θ_f (i.e. water+NAPL). The soil samples were oven dried at 105°C and passed through a 2 mm sieve. Known quantities of soil, water and oil were mixed and repacked into plastic cylinders (15 cm high and 9.5 cm in diameter); 40 different combinations of water and oil were tested, with θ_{NAPL} varying from 0.05 to 0.40 by 0.05 cm^3/cm^3 increments. A volumetric mixing model with three (soil matrix-water-NAPL) or four (soil matrix-air-water-NAPL) phases permitted conversion from a dielectric permittivity domain into a θ_f domain. The results show that, the amount of contaminant in soil can be inferred if the total volume of pore fluid θ_f and the dielectric permittivity of the contaminated soil are known. Further work will be built on this initial study, concentrating on: i) enhancing the model linkage and validating it with new laboratory results; ii) validating the developed TDR interpretation tool with field results.

Keywords: soil-NAPL-water mixtures; dielectric permittivity; mixing models.

* Corresponding author. Tel.: +39-0971-102-474
E-mail address: alessandro.comegna@unibas.it

1878-0296 © 2013 The Authors. Published by Elsevier B.V
Selection and/or peer-review under responsibility of the Scientific Committee of the Conference
doi:10.1016/j.proenv.2013.06.079

1. Introduction

Subsurface contamination of soil and groundwater with organic compounds from waste disposal sites, industrial spills, gasoline stations, mine tailings and industrial processes constitutes a serious geo-environmental problem. The detrimental effects are limited not only to deterioration of chemical, physical and mechanical properties of soils, but also constitute a real risk to human health and the well-being of other living species.

Non-aqueous phase liquids (NAPLs), are organic compounds immiscible with water. They have low solubility that may still be several orders of magnitude higher than that of acceptable drinking water standards. NAPLs can be further subdivided into those that are denser than water (DNAPLs) and those that are lighter than water (LNAPLs). Chlorinated solvents such as trichloroethylene (TCE) and tetrachloroethylene (PCE) and polychlorinated biphenyl oils (PCBs) are common examples of DNAPLs. Hydrocarbon fuels such as gasoline, kerosene and jet fuels are common LNAPL contaminants which pollute the environment extensively [1; 2].

Following a near-surface release, NAPLs penetrate the subsurface as an immiscible oil phase that migrates in response to gravity and capillary forces. This results in substantial sensitivity to the local distribution of soil and aquifer properties (e.g. permeability and porosity) beneath the source ([3]). As a result, the NAPL body (e.g. the source zone) is often expected to exhibit a complex heterogeneous distribution of both mobile pools (i.e. connected-phase accumulations) and immobile residuals (i.e. disconnected blobs and ganglia; [4]).

The remediation of contaminated soil sites requires knowledge of the contaminant distribution in the soil profile and groundwater. Methods commonly used to characterize contaminated sites are coring, soil sampling and the installation of monitoring wells for the collection of groundwater samples [4].

Given the high cost of the above methods, other non-invasive methods have been sought to extensively characterize sites and provide volume-averaged properties that support localized measurements provided by sampling and coring. Indirect detection with geophysical methods (e.g. radar, resistivity and conductivity) offers an attractive alternative [5]. In particular, the time domain reflectometry (TDR) technique has been proposed as potentially exhibiting sufficient sensitivity and lateral and vertical resolution for characterization of saturation of NAPLs (θ_{NAPL}). This is because commonly encountered NAPLs have a dielectric permittivity of 2-10 versus 81 for water, 1 for air, and 4-5 for soil mineral grains [6].

Most studies have demonstrated estimation of θ_{NAPL} essentially in saturated coarse-grained media [7; 8; 9; 6; 10; 11; 12; 13]. Little is known about the dielectric behaviour of contaminated fine-grained soils. The complexity of these soils arises due to polarization of the diffuse-double layer, whereas coarse-grained soils do not possess polarization at which most of the cited studies have been conducted. Moreover, in these studies estimation of θ_{NAPL} using TDR measurements of dielectric properties relies greatly on various mixing models [14] relating the measured dielectric permittivity to the volume fractions of the pore fluids and various soil phases such as solid, water, air and NAPLs.

New laboratory-controlled experiments are still needed to extend the above research on TDR identification of organic contaminated soils by dielectric permittivity measurements. The experimentation strategy of the present research emphasized, in a preliminary approach, the study of the potential use of TDR to monitor or map θ_f ($= \theta_w + \theta_{NAPL}$) in soil. The specific aims include: i) evaluation of correlations between θ_f in variable saturated volcanic Vesuvian soil, and dielectric permittivity and, ii) examination and validation of the mixing models provided by Francisca and Montoro [13] for predicting the dielectric permittivity of contaminated soil.

2. TDR and complex dielectric permittivity of soil

The time domain reflectometry technique is a widely accepted geophysical method to estimate the complex dielectric permittivity (ε^*) of the soil. The complex dielectric permittivity consists of two parts, a real and an imaginary part, and can be expressed by the relation of Ledieu et al.; [15]:

$$\varepsilon^* = \varepsilon' + i\left[\varepsilon'' + \frac{\sigma}{\omega\varepsilon_0}\right] \tag{1}$$

where ε^* is the complex dielectric permittivity of the medium, ε' is the real part (which represents the polarizability of the material), i is the imaginary unit (= $\sqrt{-1}$), ε'' is the imaginary part (which captures the losses due to conduction and polarization), σ (Siemens/m) is the zero frequency conductivity, ω (radians/s) is the angle frequency and ε_0 (=8.85*10^{-12} Farads/m) is the permittivity in free space.

At the highest effective frequency of the TDR Tester (200 MHz to 1.5 GHz) the complex dielectric permittivity ε^* is considered to represent the real part only (ε' , [16]). Besides, in the frequency range transmitted from the TDR instrument the ε' of most soil is almost independent of frequency.

Without introducing serious errors, under these assumptions, the propagation velocity (v) of electromagnetic waves through an homogeneous medium can be expressed as:

$$v = \frac{c}{\sqrt{\varepsilon'}} \tag{2}$$

where c(= $3 \cdot 10^8$ m/s) is the velocity of an electromagnetic wave in free space [17].

3. Materials and Methods

3.1. Experimental setup

The experimental setup consists of an excitation unit constituted by a TDR signal generator (Tektronix 1502C) and a a three-wire TDR probe, with wave guides 15 cm long, connected to the signal generator by a coaxial cable 2 m long. The reflected signals are collected by a PC-based data acquisition and processing system. The reflected signal carries the signature of the sample under study. Estimation of ε' was calculated from the signal using Win-TDR software (developed by the Soil Physics Group at Utah State University). Figure 1 gives a picture of the dielectric measurement system used in our experiment.

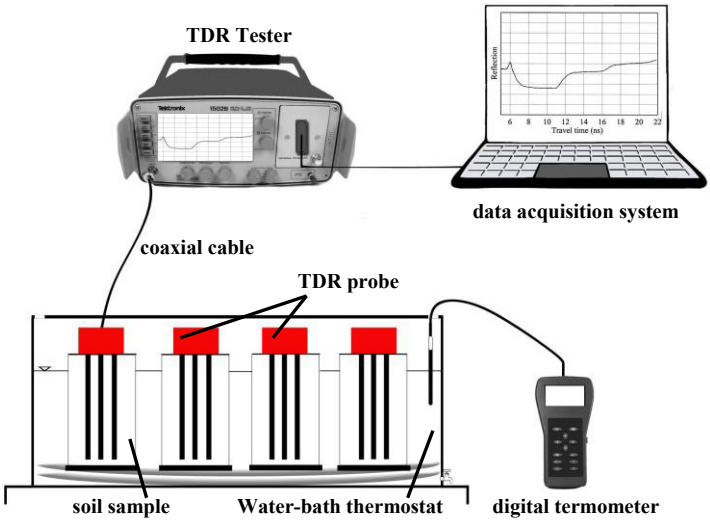

Figure 1 Experimental setup used in the experiment.

3.2. Material properties and testing procedures

The soil used for this study was sampled from an Ap horizon of a soil pedologically classified as Andosol (for details see [18]), localized in Campania region (Italy). In table 1 we have also exploited the main physico-chemical soil properties.

Table 1 Main physico-chemical properties of the soil.

Horizon	Depth (cm)	Soil texture (IUSS)				$Al_o + \frac{1}{2} Fe_o$	OC	Se
		Coarse sand %	Fine sand %	Silt %	Clay %	%	%	m^2g^{-1}
Ap	0-80	30.0	50.0	12.0	8.0	1.05	1.90	125.4

The soil texture was determined using hydrometer and sieving analysis [19]; organic content (OC) was determined by Walkley-Black method [20], The specific surface area (S_e) was determined with ethylene glycol monoethyl ether [21].

Soil samples were oven dried at 105°C and passed through a 2 mm sieve. Corn oil, a non-volatile and non-toxic LNAPL, was used as soil contaminant. The dielectric permittivity and density of the oil were 3.2 (at 25°C) and 0.905 g/cm^3 respectively. In all, there were 40 oil-contaminated soil samples, used for a full factorial analysis presented in table 2. The contaminated soil samples were shaken for 15 minutes, then kept for 24 hours in sealed plastic bags to avoid any evaporation and to ensure a uniform distribution of oil and water within the sample and good oil and water adsorption by the soil matrix. The soil is then placed in PVC soil containers of cylindrical geometry (15 cm high and 9.5 cm in diameter).

For all tests the soil was placed in the PVC containers in several steps during which it was compacted until a 1.09 g/cm^3 bulk density was attained. At each step the compacted surface was scraped to avoid the appearance of plane boundaries which give the sample a stratified behaviour responsible for parasitic reflections on the TDR signal. Soil samples were kept at a fairly constant temperature (25°C) through the TDR measurements using a water-bath thermostat.

Table 2 Combinations of moisture volume (V_w) and NAPL volume (V_{NAPL}) at fixed values of volume fraction of NAPL (β).

volumetric fluid content θ_f	volume of fluids (cm^3)	relative volume of NAPL in water: β					volumetric fluid content θ_f	volume of fluids (cm^3)	relative volume of NAPL in water: β				
		1	0.75	0.5	0.25	0			1	0.75	0.5	0.25	0
0.05	V_w	0	13	27	40	53	0.025	V_w	0	67	133	200	267
	V_{NAPL}	53	40	27	13	0		V_{NAPL}	267	200	133	67	0
0.10	V_w	0	27	53	80	107	0.30	V_w	0	80	160	240	320
	V_{NAPL}	107	80	53	27	0		V_{NAPL}	320	240	160	80	0
0.15	V_w	0	40	80	120	160	0.35	V_w	0	93	187	280	373
	V_{NAPL}	160	120	80	40	0		V_{NAPL}	373	280	187	93	0
0.20	V_w	0	53	107	160	213	0.40	V_w	0	107	213	320	427
	V_{NAPL}	213	160	107	53	0		V_{NAPL}	427	320	213	107	0

In the present study, from among the many physical models of dielectric permittivity that describe soil as a mixture of particles, water and air, the α model was used [22].

$$\varepsilon' = \left[\sum_{i=1}^{n} v_i \varepsilon_i^{\alpha} \right]^{1/\alpha} \tag{3}$$

where ε' is the permittivity of the mixture, ε_i and v_i are the permittivity and volume of the *"i"* phase respectively, the exponent α is an empirical constant related to the geometry of the grains and their spatial distribution [23; 24]. For a homogeneous and isotropic medium, α can be assumed equal to 0.5 [25] and the mixing model is then referred to as the complex refractive index model (CRIM, e.g. [26]). The CRIM model does not account for the microgeometry of the components. However, despite this limitation, and the apparent simplicity of using the CRIM model, remarkably good agreement was found in modeling the dielectric properties of geological materials [27] and soil-water-NAPL mixture [13].

For mixtures of soil saturated with water, the CRIM formula yields:

$$\varepsilon'_{sw} = \left[(1-\phi)\varepsilon'^{\alpha}_{s} + \phi\varepsilon'^{\alpha}_{w} + \phi(1-S)\varepsilon'^{\alpha}_{a} \right]^{1/\alpha} \tag{4}$$

where ε'_{sw} is the permittivity of soil-water mixture, ε'_s, ε'_w, ε'_a are the permittivities of soil particles, water and air respectively, S is the degree of saturation and ϕ is the porosity of the sample.

Similarly for soil-organic mixtures, the CRIM formula becomes:

$$\varepsilon'_{sNAPL} = \left[(1-\phi)\varepsilon'^{\alpha}_{s} + \phi S\varepsilon'^{\alpha}_{NAPL} + \phi(1-S)\varepsilon'^{\alpha}_{a} \right]^{1/\alpha} \tag{5}$$

where ε'_{sNAPL} is the permittivity of the soil-NAPL mixture and ε_{NAPL} is the permittivity of NAPL. Mixtures of soil particles, water, NAPL and air can be considered as mixtures of soil-air and water (equation 4) with soil air and NAPL (equation 5):

$$\varepsilon'_{sw-NAPL} = \left[\beta\varepsilon'^{\alpha}_{NAPL} + (1-\beta)\varepsilon'^{\alpha}_{sw} \right]^{1/\alpha} \tag{6}$$

where $\varepsilon'_{sw-NAPL}$ is the permittivity of the soil-water-NAPL mixture and β is the relative volume of NAPL (θ_{NAPL}) in water (θ_w):

$$\beta = \theta_{NAPL} / (\theta_{NAPL} + \theta_w) \tag{7}$$

4. Results and Discussion

Figure 2 shows a comparison between the measured dielectric permittivity and CRIM models (equations 4-5), fitted to the experimental data, corresponding to fully uncontaminated soil and fully contaminated soil respectively, as a function of the volumetric fluid content in the samples ($\theta_f = \theta_w$ or θ_{NAPL}).

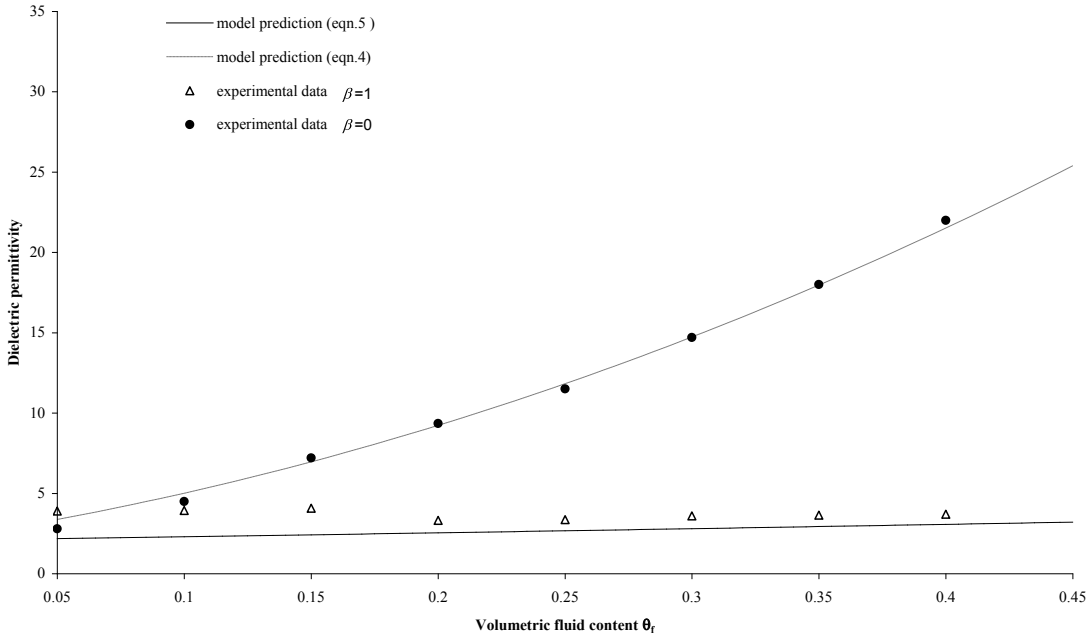

Figure 2 Effect of volumetric fluid content (θ_f) on dielectric permittivity of soil-water (ε'_{sw}) and soil-water-NAPL (ε'_{sNAPL}) mixtures.

In the CRIM model, to achieve accurate modeling, we adopt for the dielectric permittivity of the solid phase (ε'_s) a value of 4.18, measured with the immersion method [28; 29], which is, until recently the most common method for measuring ε'_s of soils: Figure 2 shows that: i) dielectric permittivity increases with volumetric content of fluids θ_f (= θ_w or θ_{NAPL}), while the presence of NAPL reduces the dielectric permittivity of the soil. The observed higher and lower dielectric permittivity values of the soil-water and soil-NAPL mixtures can be attributed here respectively to the presence of a larger amount of polar molecules in soil-water mixtures and to the non-polar nature of NAPL molecules in the soil-NAPL mixture, ii) the agreement of the CRIM model (equation 4) to the experimental data is fairly acceptable, iii) the CRIM model (equation 5) tends to underestimate the dielectric permittivity in the case of

contaminated soil with NAPL (in particular in the range $0<\theta_f<0.2$); obtained differences, even small, may arise from experimental errors and from adopted values of $\alpha=0.5$.

The model as given by Francisca and Montoro (equation 6), was then evaluated for different volume fractions of NAPL (β=0.75, 0.5, 0.25) and the resulting curves were plotted together with experimental data in figure 3 as a function of volumetric fluid content $\theta_f\left(=\theta_{NAPL}+\theta_w\right)$ in the soil samples. The model is adequate to forecast the dielectric permittivity only for values of volumetric fluid content (θ_f) greater than 0.20; notice that the slope of the curves becomes steeper as the NAPL content (β) in the pore fluids decreases.

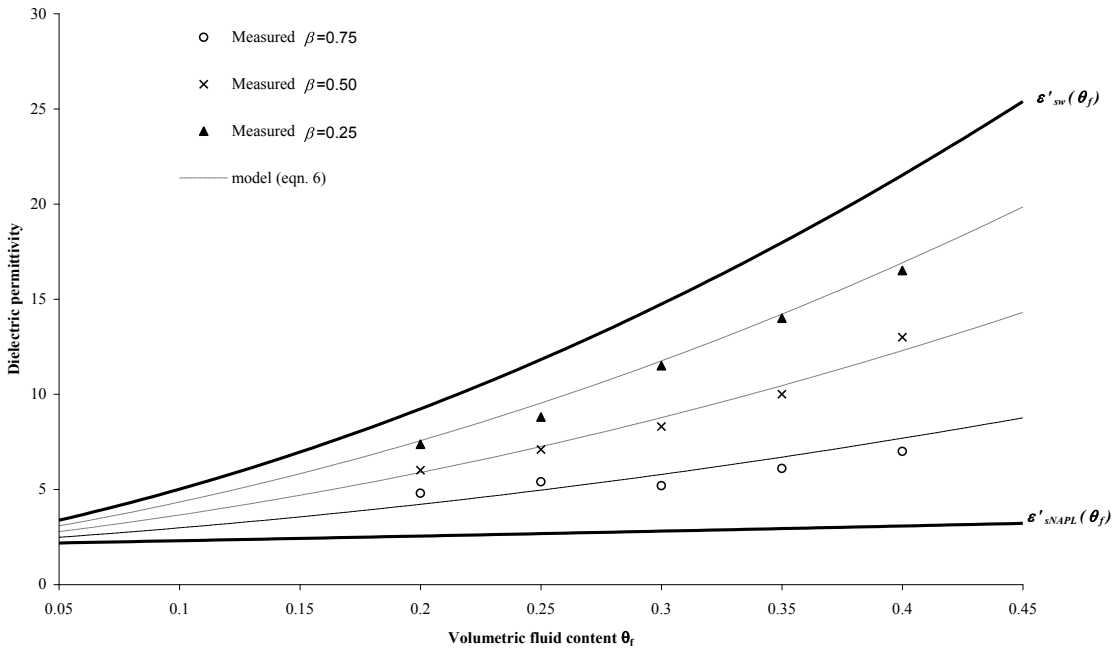

Figure 3 Dielectric permittivity of soil-water-NAPL mixtures ($\varepsilon'_{sw-NAPL}$) for different volumetric fluid contents (θ_f) and volume fractions of NAPL (β).

The volumetric content of NAPL (θ_{NAPL}), at a fixed volumetric fluid content θ_f , can be computed from equations 6 and 7, deriving $\varepsilon'^{\alpha}_{NAPL}$, $\varepsilon'^{\alpha}_{sw}$ from figure 2, and the dielectric permittivity measured in the contaminated soil $\varepsilon'_{sw-NAPL}$. Parameters can be early obtained either in laboratory or in the field. Additionally figure 3 can be very useful during an in situ remediation process to monitor the removal process.

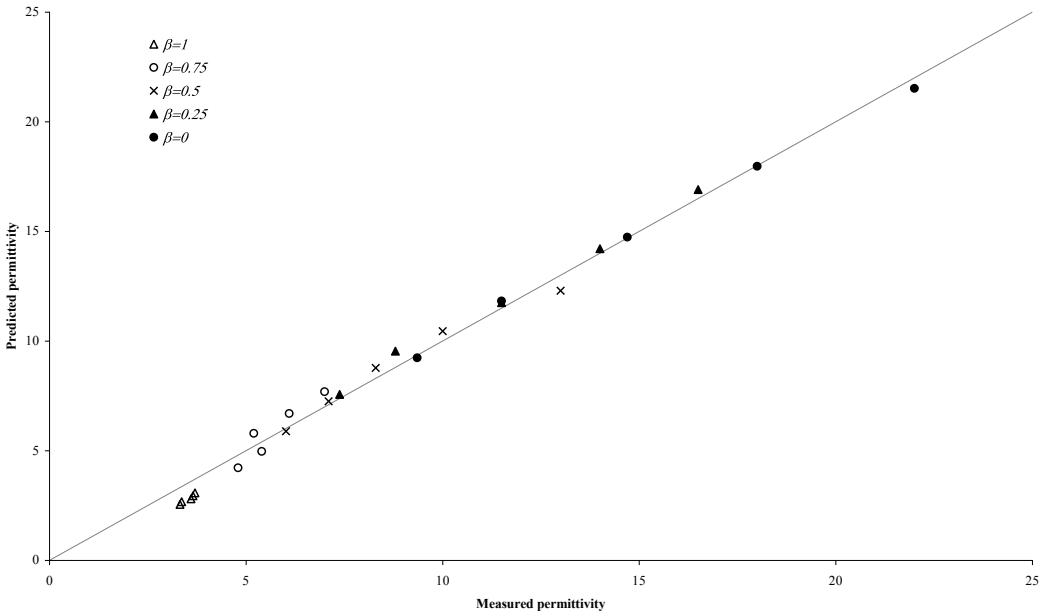

Figure 4 Relationship between calculated and measured dielectric permittivity ($\varepsilon'_{sw-NAPL}$) at different β values.

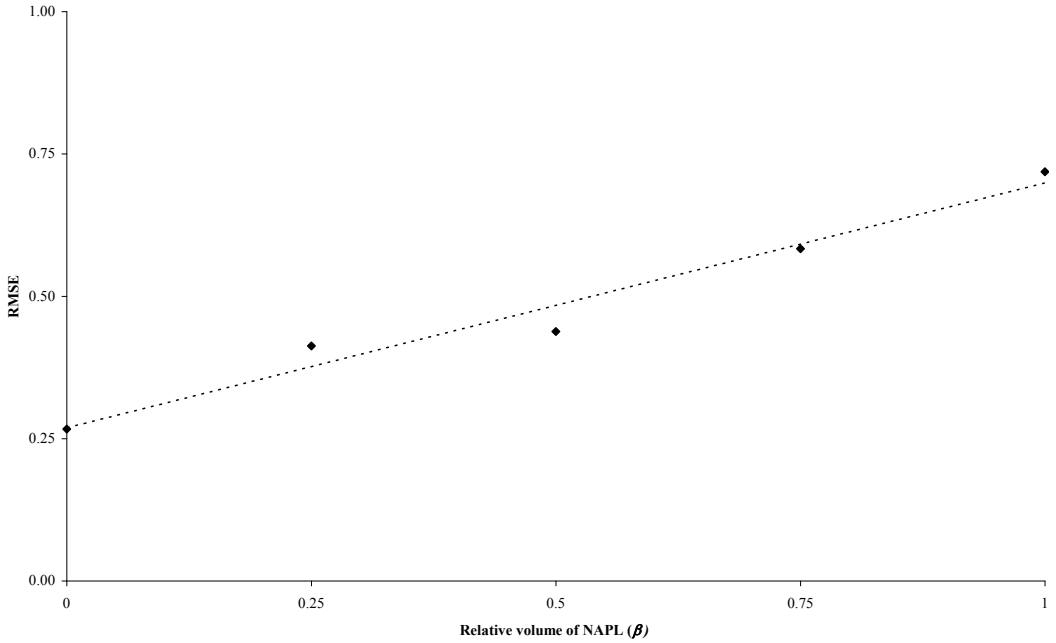

Figure 5 Relationship between the root mean square error (RMSE) and degree of volume fraction of NAPL (β).

Figure 4 presents a 1:1 plot for estimated and measured dielectric permittivity values to verify the accuracy of the dielectric mixing model (equation 6).

The model adopted, showed that the estimated dielectric permittivity values were reasonable close to the measured, meaning that with TDR methodology it is possible to achieve sufficient accuracy in predicting the presence of a contaminant, mixed with water, in the soil, that is, the root mean square error (RMSE), is 0.719, 0.584, 0.438, 0.413, 0.267 for β=1, 0.75, 0.5, 0.25, 0 respectively. Besides as may be seen from figure 5 the RMSE decreases with the decreasing of β. The observed relationship may have practical meaning for the determination of soil contaminant content: saturation of contaminated soil with water, prior to measurement dielectric permittivity using TDR, may yield better accuracy in predicting the relative volume of NAPL in water β.

5. Conclusions

From the results of our experiment it can be concluded as follows: i) the dielectric properties of contaminated soil were analyzed using mixing models extended from two to three and four components. The models that better represent the dielectric properties of contaminated soil are the models proposed by Francisca and Montoro; ii) the curves of dielectric permittivity obtained from contaminated soil and different volume of water (θ_w) and NAPL (θ_{NAPL}), were considered as upper and lower bounds respectively. The amount of contaminant in the soil can be inferred from the plots of figure 2 and 3 or with the aid of mixing models. In any case the volumetric fluid content θ_f must be known in advance; and iii) removal of contaminant inside soil pores produces an increment of soil dielectric permittivity and thus it will be directly related to contaminant reduction and replacement by the displacing fluid.

The present approach requires new experiments and data sets for model calibration in different soils. Full-scale tests should also be conducted to evaluate the performance of the technology outside a laboratory setting.

References

[1] Jury WA, Horton R. *Soil Physics*. New Jersey, John Wiley & Sons, 2004.

[2] Illangasekare HT. Flow and entrapment of Non-Aqueous-Phase Fluids in heterogeneous soil formation. In. Selim MH, Ma L, editors, *Physical nonequilibrium in soils*, Michigan, Ann Arbor Press, 1998; p417-435.

[3] Gerhard JI, Pang T, Kueper BH. Time scales of DNAPL migration in sandy aquifers. *Ground Water* 2007;**45:**147-157.

[4] Mercer JW, Cohen RM. A review of immiscible fluids in the subsurface: properties, models, characterization, and remediation. *J. Contam. Hydrol*. 1990;**6:**107-163.

[5] Redman JD, Kueper BH, Annan AP. Dielectric stratigraphy of a DNAPL spill and implications for detection with ground penetrating radar. *Ground Water Monitoring and Geophysical Methods*, 5th National Outdoor Action Conference, Natl. Ground Water Assoc., Las Vegas, Nev. 1991.

[6] Ajo-Franklin JB, Geller JT, Harris JM. A survey of the geophysical properties of chlorinated DNAPLs. *J. Appl Geophys* 2006;**59**:177-189.

[7] Redman JD, DeRyck SM. *Monitoring non-aqueous phase liquids in the subsurface with multilevel time domain reflectometry probes. Proc Symp. on Time Domain Reflectometry in Environmental, Infrastructure, and Mining Applications*, Evanston, IL. Spec. Publ. SP19-94. U.S. Bur. of Mines, Washington, DC, 1994.

[8] Chenaf D, Amara N. Time domain reflectometry for the characterization of diesel contaminated soils. *Proc. Second Int. Symp. and Workshop on Time Domain Reflectometry for Innovative Geotechnical Applications* (5-7 September 2001), Infrastructure Technology Institute, Northwestern University, Evanston, Illinois, USA, 2001.

[9] Persson M, Berndtsson R. Measuring nonaqueous phase liquid saturation in soil using time domain reflectometry. *Water Resour. Res* 2002;**38**, doi: 10.1029/2001WR000523.

[10] Haridy SA, Persson M, Berndtsson R. Estimation of LNAPL saturation in fine sand using time-domain reflectometry. *Hydrological Sciences*, 2004;**49:**987-1000.

[11] Moroizumi T, Sasaki Y. Estimating the nonaqueous-phase liquid content in saturated sandy soil using amplitude domain reflectometry. *Soil Sci. Soc. Am. J.* 2006;**72**:1520-1526.
[12] Mohamed AMO, Said RA. Detection of organic pollutants in sandy soils via TDR and eigendecomposition. *J. Contain. Hydrol*. 2005;**76**:235-249.
[13] Francisca M, Montoro MA. Measuring the dielectric properties of soil-organic mixtures using coaxial impedance dielectric reflectometry. *Journal of Applied Geophysics* 2012;**80**;101-109.
[14] van Dam RL, Borchers B, Hendrickx JMH. *Methods for prediction of soil dielectric properties: a review*. 2005, available on http://www.ees.nmt.edu/hydro/landmine.
[15] Ledieu J, De Bidder P, De Clerck P, Dautrebande S. A method of measuring soil moisture by time-domain reflectometry. *J. Hydrol*. 1986;**88**:319-328.
[16] Heimovaara TJ, Bouten W, Verstraten JM. Frequency domain analysis of time domain reflectometry waveforms, 2, A four-component complex dielectric mixing model for soils, *Water Resour. Res*. 1994;**30**:201-210.
[17] Topp CG, Davis JL, Annan AP. Electromagnetic determination of soil water content: measurements in coaxial transmission lines. *Water Resour. Res*. 1980;**16**:574-582.
[18] Severino G, Comegna A, Coppola A, Sommella A, Santini A. Stochastic analysis of a field-scale unsaturated transport experiment. *Adv. Water Resour.* 2010;**33**:1188-1198.
[19] Day PR. Particle fractionation and particle-size analysis. In Black CA, editor, *Methods of Soil Analysis, Part 1*, Madison, American Society of Agronomy, 1965; p.545-567.
[20] Allison LE. Organic carbon. In Klute A, editor, *Methods of Soil Analysis, Part 1*, Madison, Agron. Monograph, vol 9, ASA and SSSA, 1965; p.1367-1378.
[21] Carter DL, Mortland MM, Kemper WDM. Specific Surface. *Methods of Soil Analysis, Part I.* Physical and Mineralogical Methods-Agron, Monograph vol. 9 (2nd Edition), ASA and SSSA, Madison, 1986; p.413-423.
[22] Roth K, Schulin R, Fluhler H, Attinger W. Calibration of time domain reflectometry for water content measurements using a composite dielectric approach. *Water Resour. Res* 1990;**26**:2267-2273.
[23] Hilhorst MA. *Dielectric characterisation of soil*. PhD dissertation, Wageningen Agricultural University, 1998.
[24] Coppola A, Dragonetti G, Comegna A, Lamaddalena N, Caushi B, Haikal MA, Basile A. Measuring and modeling water content in stony soils. *Soil Till. Res.* 2013;**128**:9-22.
[25] Alharti A, Lange J, Whitaker E. Immiscible fluid flow in porous media: Dielectric properties. *J. Contam. Hydrol*. 1986;**1**:107-118.
[26] Huisman JA, Hubbard SS, Redman JD, Annan AP. Measuring soil water content with ground penetrating radar: A review, *Vadose Zone J.* 2003;**2**:476-491.
[27] Knight R. ground penetrating radar for environmental applications. *Annu. Rev. Earth Planet Sci*. 2001;**29**:229-255.
[28] Robinson DA, Jones SB, Wraith JM, Or D. A review of advances in dielectric and electric conductivity measurements using time domain reflectometry, *Vadose Zone J.* 2003;**2:**444-475.
[29] Kameyama K, Miyamoto T. Measurement of solid phase permittivity for soils by time domain reflectometry. *European Journal of Soil Science* 2008;**59**:1253–1259.